



Preparation and dielectric relaxation of a novel ionocellulose derivative

Ahmed Salama, Fathia Mohamed, Peter Hesemann

► To cite this version:

Ahmed Salama, Fathia Mohamed, Peter Hesemann. Preparation and dielectric relaxation of a novel ionocellulose derivative. Carbohydrate Polymer Technologies and Applications, 2021, 2, pp.100087. 10.1016/j.carpta.2021.100087 . hal-03233368

HAL Id: hal-03233368

<https://hal.science/hal-03233368>

Submitted on 4 Jun 2021

HAL is a multi-disciplinary open access archive for the deposit and dissemination of scientific research documents, whether they are published or not. The documents may come from teaching and research institutions in France or abroad, or from public or private research centers.

L'archive ouverte pluridisciplinaire **HAL**, est destinée au dépôt et à la diffusion de documents scientifiques de niveau recherche, publiés ou non, émanant des établissements d'enseignement et de recherche français ou étrangers, des laboratoires publics ou privés.

Preparation and dielectric relaxation of a novel ionocellulose derivative

Ahmed Salama^{1,2*}, Fathia Mohamed³ and Peter Hesemann^{1*}

¹ICGM, Univ Montpellier-CNRS-ENSCM, Montpellier, France

²Cellulose and Paper Department, National Research Centre, 33 El-Behouth St.,
Dokki, P.O. 12622, Giza, Egypt

³Spectroscopy Department, Physics Research Division, National Research Centre, 33
El-Bohouth St., 12622, Dokki, Giza, Egypt

*corresponding authors

Keywords

Cellulose derivatization; tosylcellulose; Ionic liquids; Dielectric relaxation;
conductivity

Abstract

A new water-soluble ionocellulose material bearing imidazolium tosylate groups was synthesized in a two-step sequence from cellulose, and the electrical conduction properties of this bio sourced polyelectrolyte were investigated. First, tosylcellulose was prepared from neat cellulose and tosyl chloride in the ionic liquid 1-Butyl-3-methylimidazolium chloride [BMIM]Cl. Then, the ionocellulose containing imidazolium tosylate grafts was synthesized by reacting tosylcellulose and 1-methylimidazole. Both tosylcellulose and ionocellulose were characterized by different analytical techniques including elemental analysis, ^{13}C NMR and FT-IR spectroscopy as well as thermogravimetric analysis. We then compared the dielectric relaxation of neat cellulose with ionocellulose. For both samples, two secondary relaxations were identified at low temperature. These two relaxations became faster in ionocellulose containing imidazolium tosylate grafts. At higher temperatures ($T > \text{room temperature}$), the conductivity is markedly dominated by ionic motions. This work opens new perspectives for preparing a new category of ionocellulose derivatives which are expected to find applications in energy storage technologies and for the elaboration as novel high-performance film dielectric capacitors.

Highlights

- Straightforward cellulose derivatization using ionic liquid reaction media
- Synthesis of water-soluble ionocellulose bearing imidazolium tosylate grafts.
- Investigation of the dielectric properties of imidazolium functionalized ionocellulose
- Structure-property relationship of ionocellulose as a novel type of poly(ionic liquid)

Introduction

Cellulose, the most abundant polymer on Earth, displays some interesting properties such as biocompatibility, biodegradability, and thermal stability which makes it highly attractive as renewable resource for various applications, for example in the biomedical field or in energy storage (Salama, 2019; Wang, Gurau, & Rogers, 2012). However, one of the major limitations for applying cellulose in sustainable technologies is the lack of efficient strategies for its processing, as cellulose is insoluble in water and conventional organic solvents (Salama, Neumann, Günter, & Taubert, 2014). New approaches for efficient cellulose processing and derivatization are therefore highly desirable (Salama, Abou-Zeid, Cruz-Maya, & Guarino, 2020), and particularly the generation of novel soluble cellulose derivatives is a field of intense research activity (Elschner & Heinze, 2015; Rong et al., 2019). In particular, cellulose derivatization on the C6 position of the D-anhydroglucopyranose units via its functionalization with good leaving groups offers multiple possibilities for cellulose modification. In this respect, the formation of tosylcellulose and its subsequent nucleophilic substitution with butylamine and pyridine was reported (C. Liu & Baumann, 2005). Another study showed that cellulose derivatives such as 6-deoxy-6-bromo-cellulose allow accessing amino-functionalized cellulose derivatives via regioselective substitution (S. Liu, Liu, Esker, & Edgar, 2016).

The p-toluene sulfonic acid ester of cellulose, tosylcellulose, appears as a highly versatile intermediate for the synthesis of a large variety of new cellulose derivatives via nucleophilic substitution reactions (Schmidt, Liebert, & Heinze, 2014). The tosyl moiety is an excellent leaving group and can be substituted by various nucleophiles such as halides, pseudo-halides (azide, thiocyanate,...) or amines, to access novel 6-deoxy-6-functionalized cellulose derivatives (Gericke et al., 2012). For example, new water soluble cellulose derivatives can be obtained from tosylcellulose through nucleophilic substitution with aminoalkyl acid derivatives (El-Sayed, El-Sakhawy, Hesemann, Brun, & Kamel, 2018). Hence, nucleophilic substitution reactions with tosylcellulose open up new pathways for cellulose modification in view of the elaboration of functional materials from renewable resources.

The tosylation performed in homogeneous media allows achieving a high degree of substitution (DS) and uniform distribution of the tosyl moieties along the cellulose chains (Schmidt et al., 2014). Typically, the homogeneous tosylation of cellulose can

be achieved in *N,N*-dimethylacetamide (DMAc)-LiCl with *p*-toluenesulfonyl chloride in the presence of triethylamine. This procedure produces tosylcellulose that is soluble in a variety of solvents (Rahn, Diamantoglou, Klemm, Berghmans, & Heinze, 1996). However, the tosylation of cellulose is not a trivial process, and other strategies for more sustainable synthesis processes for tosylcellulose were investigated (El-Sayed et al., 2018). In this context, cellulose derivatization in ionic liquid (IL) media appears as a promising strategy to access for cellulose modification.

Ionic liquids were reported as efficient solvents for the solubilization of polysaccharides and more specifically for cellulose. Homogeneous solutions of cellulose dissolved in IL media allowed accessing a variety of chemical cellulose modifications and gave rise to new cellulose derivatives (Salama & Hesemann, 2020a). Homogeneous cellulose solutions in ionic liquids have been applied for the preparation novel cellulose derivatives, mainly of esters of organic and inorganic acids (Wu et al., 2004). The preparation of tosylcellulose in ionic liquids as an intermediate for further conversion into different cellulose derivatives has already been reported (Gericke et al., 2012).

In this work, we particularly focused on the derivatization of cellulose with ionic imidazolium groups. Polysaccharides bearing positive charges show remarkable physical and chemical properties and were suggested for promising applications such as adsorption (Salama & Hesemann, 2018b, 2018a) and biomaterials (Salama, Hasanin, & Hesemann, 2020; Salama & Hesemann, 2020b). Moreover, these biopolymers can bind electrostatically with other anionic biomolecules such as nucleic acids and some proteins to form polyelectrolyte complexes for therapeutic applications. For example, chitosan, the most common cationic polysaccharide, has the ability to improve permeation of peptide drugs across mucosal epithelia (Thanou, Verhoef, & Junginger, 2001). It can encapsulate anionic nucleic acids or certain proteins and protect them from degradative enzymes (Lai & Lin, 2009). Moreover, chitosan bearing quaternized ammonium derivatives shows permanent positive charge, high solubility in a large range of pH values, and promising ability to enhance absorption of hydrophilic drugs (Thanou et al., 2001).

In this work, we focused on the formation of a cellulose derivative bearing covalently grafted cationic imidazolium groups starting from cellulose. For this purpose, we firstly investigated the synthesis of tosylcellulose in ionic liquid reaction medium. This method efficiently produced highly soluble tosylcellulose that was then reacted with methyl imidazole to produce a novel cellulose derivative, namely ionocellulose

containing imidazolium tosylate grafts . Our synthetic strategy is highly sustainable as it involves the elaboration of new functional materials from cellulose, the most abundant natural resource, using green solvents, *i.e.* ionic liquids and under mild reaction conditions. We then focused on the investigation of the conduction properties of this bio-sourced polyelectrolyte. The dielectric response of the ionocellulose was investigated in the frequency range 0.1 Hz-10⁷ Hz and the temperature range T = 203 K – 363 K. The influence of the imidazolium tosylate on the dielectric response of the cellulose was compared to that of neat cellulose. The dc and ac electrical conductivity are discussed.

2. Materials and Methods

2.1. Materials

Microcrystalline cellulose powder, p-toluenesulfonyl chloride and 1-methylimidazole were supplied from Sigma Aldrich. 1-Butyl-3-methylimidazolium chloride [BMIM]Cl was purchased from IoLiTec. All other chemicals of analytical grade were used as received.

2.2. Syntheses

Tosylation of cellulose in a mixture of [BMIM]Cl and pyridine.

In a round bottom flask, 2.0 g of cellulose (12.34 mmol anhydroglucose units, AGU) were stirred with 18 g [BMIM]Cl at 80°C for 16 h. After complete dissolution, the solution was cooled to 25°C and 10 ml pyridine were added under vigorous stirring. Then, a solution of 7.06 g *p*-toluenesulfonyl chloride (3 mol per mol AGU) in 10 ml pyridine was added dropwise to the cellulose/[BMIM]Cl/pyridine mixture within 5 minutes at room temperature. After stirring at 25°C for 12 h, the reaction mixture was poured into 350 ml of ethanol, resulting in the formation of a precipitate. The obtained product was separated by filtration, washed with ethanol, water, and again three times with ethanol (100 ml each), and finally dried under vacuum at 60°C. Yield: 3.2 g. Elemental analysis found for cellulose (%): C 42.9, H 6.4, N 0.0, S 0.0; for tosylcellulose (%): C 45.3, H 5.2, N 0.03, S 10.2.

Preparation of ionocellulose containing imidazolium tosylate grafts.

1 g tosylcellulose (3.56 mmol modified AGU, $DS_{\text{tosyl}} = 1.02$) was dissolved in 5 ml DMSO and 3.1 g methyl imidazole (3.8 mmol) were added. After 24 h stirring at 100°C, the reaction mixture was cooled to room temperature and poured into 50 ml ethyl acetate. The resulting precipitate was separated, washed five times with ethyl acetate (25 ml each), and finally dried under vacuum at 60°C. Yield (cellulose containing imidazolium tosylate): 1.3 g. Elemental analysis found (%): C 44.8, H 4.5, N 5.5, S 4.9.

2.3. Characterization methods.

Elemental analysis. EA was done with an Elemental Vario Micro Cube apparatus.

FT-IR Spectroscopy. The attenuated total reflectance Fourier transform infrared (ATR-FTIR) spectra of materials were obtained using a Thermo Nicolet FT-IR Avatar 320 with a diamond crystal. Spectra were recorded from 500 to 4000 cm^{-1} .

Thermogravimetric Analysis. TGA measurements were carried out with a NETZSCH STA 409 PC instrument. All materials were burned under oxygen atmosphere between 25 and 900 °C at a heating rate of 5°C/min.

Liquid NMR spectroscopy. ^{13}C NMR spectra in solution were recorded on a Bruker Avance 400 spectrometer at room temperature. Deuterated dimethyl sulfoxide (DMSO-d_6) was used as solvent for liquid NMR experiments and chemical shifts are reported as δ values in parts per million relative to tetramethylsilane.

Dielectric properties. For the dielectric measurements, an Alpha-A machine from novocontrol was utilized in the frequency range 10^{-1} to 10^7 Hz and at temperatures ranging from 220 K to 363 K. The temperature stability was better than ± 0.1 K as a Quatro controller system using pure nitrogen as a heating agent was employed.

3. Results and discussions

Cellulose dissolution in ionic liquids has already been described in the literature (Wang et al., 2012). It has been reported that tosylcellulose can be prepared from cellulose, in homogenous ionic liquid media, using tosyl chloride and in the presence of triethylamine. Substitution degrees up to 0.84 indicate a predominant tosylation of the primary hydroxyl group on the C6 position of the D-anhydroglucopyranose units (AGU) (Gericke et al., 2012). In the current work, tosylation of cellulose in homogeneous [BMIM]Cl ionic liquid media and in the presence of pyridine proceeded smoothly without any precipitation or phase separation during the reaction. The formation of the imidazolium tosylate based ionocellulose was achieved in a second reaction step through direct nucleophilic substitution of tosyl groups with methyl imidazole as depicted in scheme 1.

Elemental analysis and DS

The tosylation reaction and the subsequent formation of imidazolium based ionocellulose were firstly monitored *via* elemental analysis (EA). EA allows for a quantitative determination of the tosylation reaction and the subsequent quaternization reaction with methyl imidazole via the determination of the sulphur and nitrogen content for the materials. The results of the EA measurements for cellulose, tosylcellulose and ionocellulose containing imidazolium tosylate are given in table 1.

Table 1 Results of EA experiments with cellulose, tosylcellulose and ionocellulose

	C	H	S	N
Cellulose	42.9	6.4	n.d.	n.d.
Tosylcellulose	45.3	5.2	10.2	0.03
Ionocellulose	44.8	4.5	4.9	5.5

The results of elemental analysis measurements reflect the chemical modification of the cellulose derivatives during the two polymer analogous reactions. Whereas neat cellulose is constituted only of the three elements C, H and O, the tosylcellulose and ionocellulose contain significant quantities of S (tosylcellulose) and both S/N (ionocellulose), indicating the successful incorporation of tosyl groups and the subsequent quaternization reaction. The degree of tosyl substitution (DS_{Tos}) was

determined by sulfur analysis and calculated according to equation (1) (Heinze, Talaba, & Heinze, 2000):

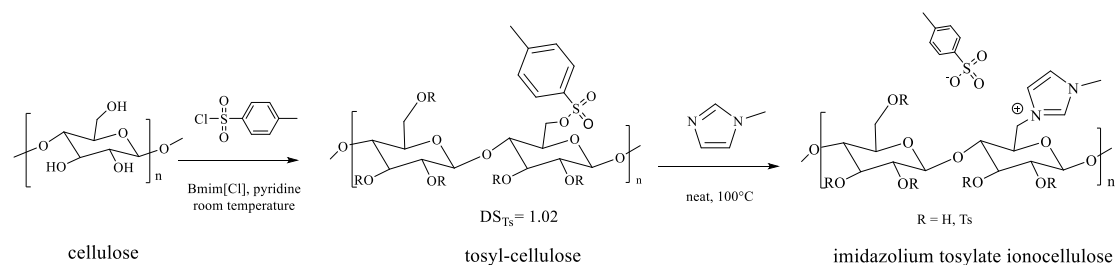
$$DS_{Tos} = M_{AGU} \cdot W_s(\%) / M_s \cdot 100 (\%) - M_{Ts} \cdot W_s(\%) \quad (1)$$

where M_{AGU} is the molar mass of the anhydroglucose unit (AGU) = 162.05 g/mol, M_s is the molar mass of sulfur = 32.065 g/mol, M_{Ts} is the molar mass of the tosyl group = 155.02 g/mol, and W_s is the weight % of sulfur = 0.8788. The obtained tosylcellulose has degree of tosyl substitution $DS = 1.02$, indicating the complete tosylation of the C6 carbon centers of the anhydroglucose units as depicted in scheme 1.

Cellulose containing imidazolium tosylate showed high percentage of nitrogen and sulphur (5.49 and 4.89%, respectively). These results give a first indication for the successful formation of imidazolium moieties supported on cellulose with tosylate as counter anion. The slight excess of nitrogen with respect to the sulphur content in the ionocellulose after nucleophilic substitution reaction with methyl imidazole may indicate a partial loss of tosylate anions during work-up.

It has to be pointed out that the dissolution properties of the cellulose derivatives are strongly modified in the course of the tosylation/quaternization reactions. Neat cellulose is only soluble in IL media, but not in organic solvents. Tosylcellulose is soluble in organic solvents such as DMSO, DMF and DMA, and the ionocellulose containing imidazolium tosylate is water-soluble.

Besides these macroscopic differences, we followed the modification of the thermal and spectroscopic properties in the course of the cellulose derivatization reaction *via* liquid ^{13}C NMR and FT-IR spectroscopy and thermogravimetric measurements.



Scheme 1: Synthesis scheme of cellulose imidazolium tosylate

IR spectroscopy

The formation of tosylcellulose and ionocellulose containing imidazolium tosylate was confirmed by FT-IR spectroscopy. The FT-IR spectra of neat cellulose (A), tosylcellulose (B) and ionocellulose containing imidazolium tosylate (C) are given in figure 1.

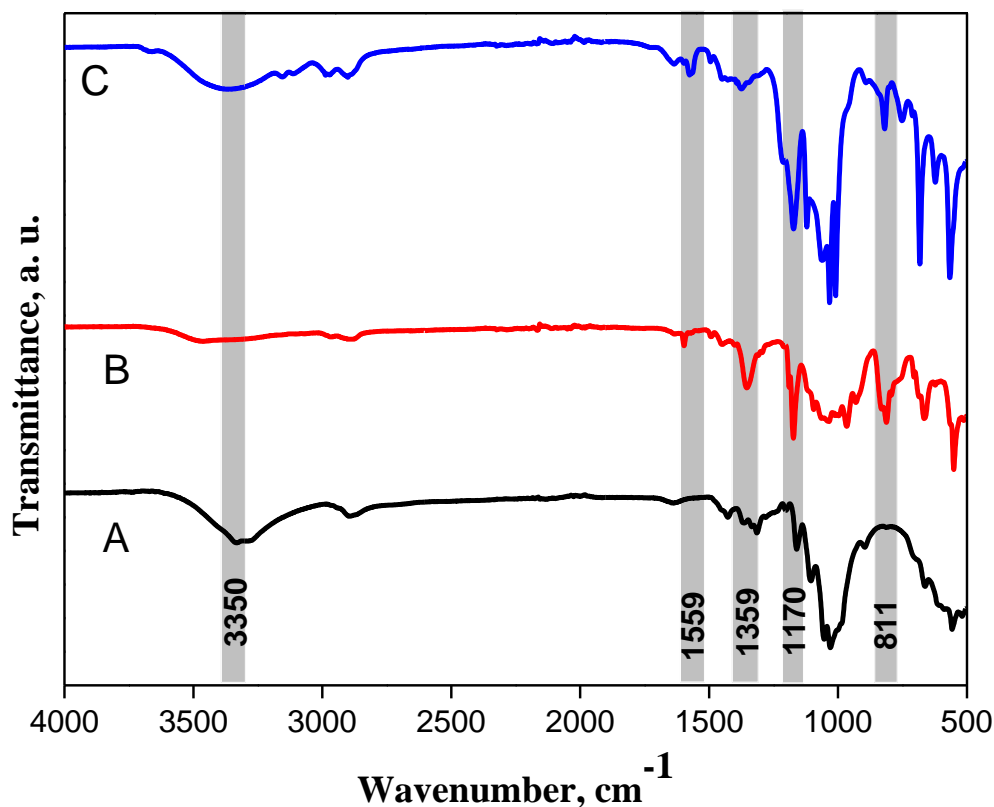


Figure 1: FT-IR spectra of neat cellulose (A), tosylcellulose (B) and imidazolium tosylate containing ionocellulose (C).

Neat cellulose exhibited absorption bands at 3327, 2888, 1427, and 1022 cm^{-1} , which can be assigned to the OH, CH_2 , CH symmetrical deformation, and C-O-C stretching vibration of cellulose, respectively (Salama & El-Sakhawy, 2016). After tosylation, additional bands can be found in the spectrum of tosylcellulose: The characteristic bands of the tosyl group were assigned at 811 cm^{-1} ($\nu \text{ S-O-C}$), 1170 cm^{-1} ($\nu_s \text{ SO}_2$), 1359 cm^{-1} ($\nu_{as} \text{ SO}_2$) and 1559 cm^{-1} ($\nu \text{ C=C}_{\text{aromatic}}$) (figure 1, B) (Koschella, Hartlieb, & Heinze, 2011). Moreover, the absorption at ca. 3350 cm^{-1} is significantly reduced indicating the lower content of hydroxyl groups in this material. Finally, the FT-IR spectrum of ionocellulose containing imidazolium tosylate shows a new absorption

band at 1560 cm^{-1} that can be assigned to C-N stretch vibration of the imidazolium rings, thus indicating successful formation of 1-methylimidazolium groups via quaternization reactions. Besides, the adsorption bands characteristic of the tosyl group are still visible in the spectrum of the ionocellulose, suggesting the presence of tosylate as counter anion for imidazolium cations.

Liquid ^{13}C NMR spectroscopy

The ^{13}C liquid NMR spectrum of tosylcellulose in deuterated DMSO is given in figure 2a. It was possible to record the NMR spectrum of tosylcellulose in solution as the polymer is readily soluble in various organic solvents. The spectrum of tosylcellulose shows signals at 128.1, 130.7, 132.5 and 145.6 ppm that can be assigned to aromatic carbons of the tosylate group. The signal at 102.5 ppm corresponds to C1 carbon centers in the anhydroglucose unit. Moreover, the signals in the area of 70-81 ppm can be attributed to the C2, C3, C4 and C5 of anhydroglucose units. The signals at 69.1 ppm can be attributed to the tosylated C6 marked as C6S. The signal of at 21.4 ppm can be assigned to the methyl group of tosylate. Finally, the weak signal at 44.8 ppm may indicate the presence of a small amount of chlorinated groups. Liquid ^{13}C NMR spectroscopy therefore confirms the successful tosylation of cellulose.

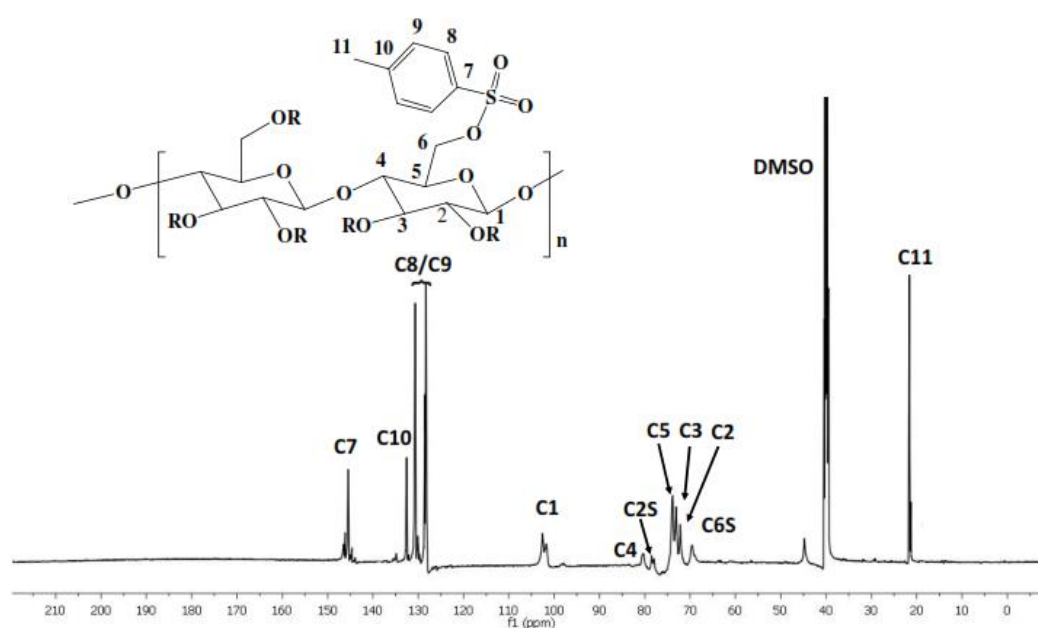


Figure 2a: ^{13}C NMR spectrum of tosylcellulose (solvent: DMSO-d_6).

Further changes can be observed in the spectrum of the ionocellulose. In the spectrum of cellulose containing imidazolium tosylate grafts, an additional signal at 35.8 ppm can be assigned to N-CH_3 while the signal at 49.3 ppm may be assigned to the methylene group neighboring the imidazolium grafts. This is in line with the complete disappearance of the signal related the $\text{CH}_2\text{-Tos}$ groups after the quaternization reaction. The new signals at 137.1, 139.5 and 142.4 ppm can easily be attributed to the grafted

imidazolium rings. The signals of tosylate counter anions are still present, together with the signals of the cellulose backbone. Hence, ^{13}C NMR spectroscopy gives clear evidence for the successful formation of ionocellulose containing imidazolium tosylate grafts, but some small signals in the aliphatic region point some side reactions during the quaternization.

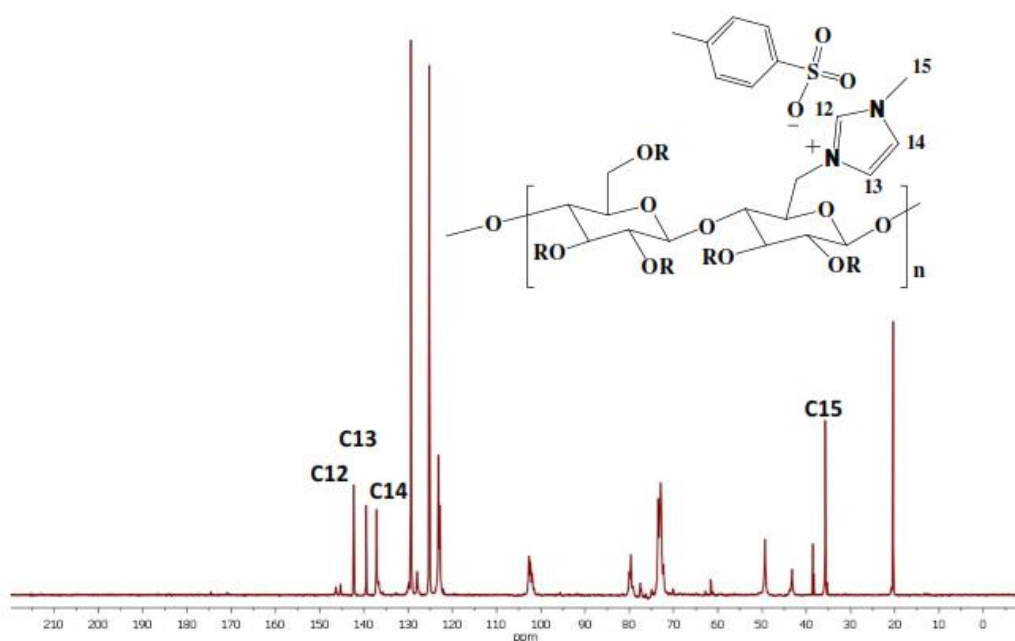


Figure 2/b: ^{13}C NMR spectrum ionocellulose containing imidazolium tosylate (solvent: D_2O)

Thermogravimetric analysis

The TGA thermograms for cellulose, tosylcellulose and ionocellulose containing imidazolium tosylate grafts are displayed in figure 3. In all materials, the weight losses can be separated into three main temperature regions, designed as regions I, II and III. From room temperature to 120°C (region I), the weight loss ranging from 3.1 to 5.2 %, may be attributed to the elimination of physically adsorbed water. The amount of physically adsorbed water is significantly higher in cellulose containing imidazolium tosylate compared to cellulose and tosylcellulose. This difference may be due to the higher hygroscopicity of this polymer. In region II ($120 - 350^\circ\text{C}$), a sharp weight loss indicates the thermal degradation of the hydrocarbon backbone of cellulose and its

derivatives. The cellulose derivatives, tosylcellulose and ionocellulose, start the degradation process at significantly lower temperatures ($\sim 175^{\circ}\text{C}$) compared to neat cellulose where the degradation takes place starting from 270°C . At the end of the region II (350°C), the weight loss reached 72.5, 55.7 and 51% for cellulose, tosylcellulose and ionocellulose containing imidazolium tosylate, respectively. Above temperatures of 350°C (region III), we observed a complete decomposition and total mass loss of the materials, thus suggesting the absence of inorganic impurities in all materials. Complete mass loss was observed at 500°C for neat cellulose and at 600°C for the two cellulose derivatives, indicating that the incorporation of functional groups containing heteroelements (N, S) may increase the thermal stability of the formed materials. Our results are therefore in line with former works, reporting that introducing cationic moieties may improve the thermal stability and water solubility of cellulose derivatives (S. Liu et al., 2016).

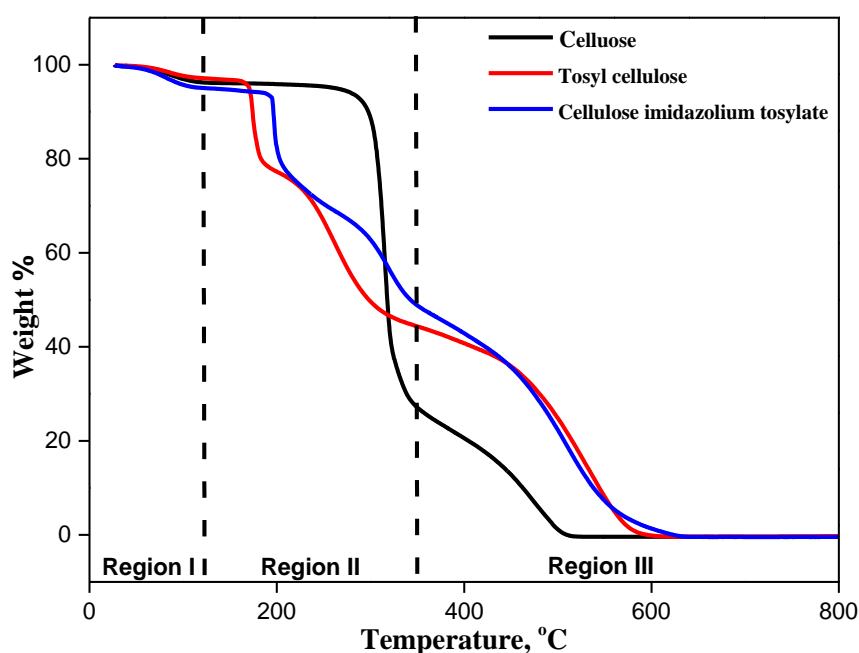


Figure 3: TGA plots of cellulose, tosylcellulose and cellulose containing imidazolium tosylate (air flux, heating ramp $5^{\circ}\text{C}/\text{min}$)

3.3 Dielectric spectroscopy

Dielectric spectroscopy is a valuable tool for monitoring the polarity of dense network with strong polar interactions or to display the charge transportation mechanism in polymers containing electric charges (polymer electrolytes) (Wieland et al., 2019). It is often considered as a complementary method to viscosimetry (Mohamed et al., 2018), neutron scattering (Nusser, Schneider, & Richter, 2011) and nuclear magnetic resonance (NMR) spectroscopy (Hofmann et al., 2012).

Figure 4a shows the dielectric loss spectra of neat cellulose. Two relaxation processes can be distinguished: the slower one, labeled as γ - process, can be observed at temperatures below -30°C (243 K). The process is completely covered by the conductivity contribution at higher temperature, which is defined by the solid line. Upon cooling, the γ -relaxation leaves the acquisition window and the other faster relaxation labelled β -relaxation becomes prevailing. The presence of these two processes in polysaccharides were previously reported (Einfeldt, Meißner, & Kwasniewski, 2001; Jafarpour, Dantras, Boudet, & Lacabanne, 2007, 2008). As described, the β -relaxation reflects the local motions within the monomeric AGU units building the polysaccharide within the chains of polysaccharides and has an intermolecular character (Kaminski et al., 2009), whereas the γ -process is associated to localized cooperative molecular mobility of the cellulose main chain, and is concluded to have thermal history sensitivity of intermolecular nature and has properties mimicking the structural α -process (Kaminski et al., 2008, 2009).

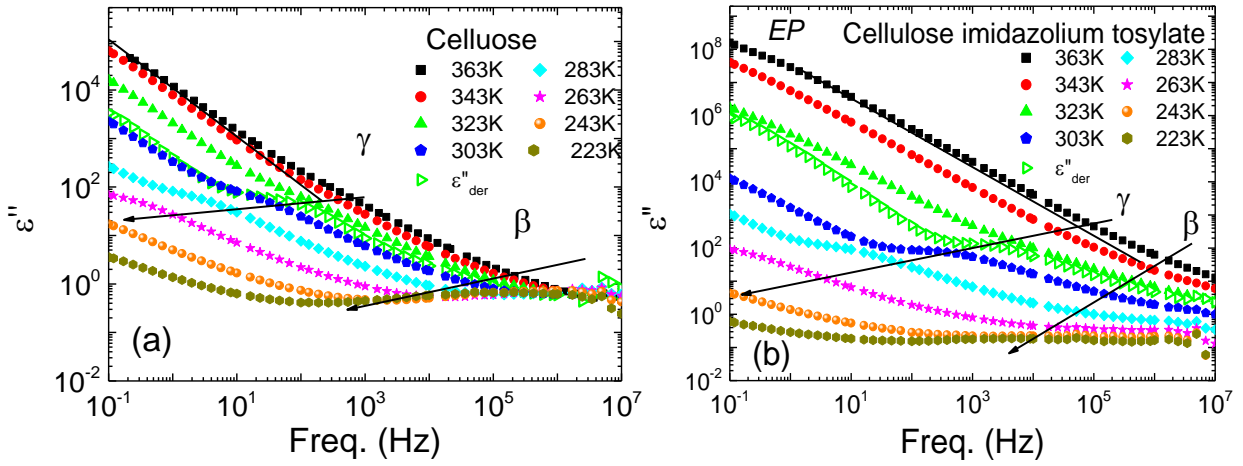


Figure 4: Dielectric imaginary part (loss) as a function of frequency of (a) cellulose and (b) ionocellulose containing imidazolium tosylate at temperatures as indicated; solid lines refers to a $\varepsilon''(\nu) \propto \nu^{-1}$ dependency. Open symbols: the reproduced $\varepsilon''_{\text{der}}$ along eq. 2.

The dielectric loss spectrum of ionocellulose containing imidazolium tosylate grafts is displayed in figure 4b. The two γ - and β -relaxations can again be observed, but they are shifted to higher frequency (*cf.* figure 5b). This result is in accordance with a plasticizer effect (Bao, Long, & Vergelati, 2015; Petridis et al., 2014; Pötzschner et al., 2017). A decrease of the viscosity of cellulose was found in the presence of ionic liquids, in particular, 1-ethyl-3-methylimidazolium diethyl phosphate (Minnick, Flores, & Scurto, 2017). At low frequency, a slight bending from the line reflecting the conductivity contributions can be observed. This may refer to the electrode polarization (*EP*). This phenomenon describes the fluctuations of accumulated charges at the surface of the electrode (Sawada, 2007). One should note here that the strength of the process is slightly higher compared to that in case of neat cellulose. This may give an indication that the amorphous character is enhanced in the ionocellulose. Previous studies showed that ionic liquid disrupts the crystalline structure of cellulose but keeps its amorphous part (Kadokawa, Murakami, & Kaneko, 2008). As already stated, the γ -process is completely masked with the contribution of the conductivity at higher temperature. To separate the processes, we reproduced the imaginary part ($\varepsilon''_{\text{der}}$) from the permittivity (ε') (Gabriel, Pabst, Helbling, Böhmer, & Blochowicz, 2018; Wübbenhorst & van Turnhout, 2002):

$$\varepsilon_{der}''(\omega) = \frac{-\pi}{2} \frac{d\varepsilon'}{d \ln \omega} \quad (2)$$

Doing so, the process is separated in good approximation (see for example the data at $T = 323\text{K}$ in Figure 4). In Figure 5, the separated ε_{der}'' as well as the measured ε'' data are fitted using two Havriliak-Negami (HN) functions together with the conductivity contribution along (Bottcher, 1973):

$$\widehat{\varepsilon}(\omega) = \frac{\Delta\varepsilon}{(1 + (i\omega\tau_0)^a)^b} - i \frac{\sigma}{\varepsilon_0 \omega} + \varepsilon_\infty \quad (3)$$

with $\widehat{\varepsilon}(\omega)$ is the complex dielectric function, σ denotes the conductivity, and ω is the angular frequency. Also, a and ab are the power-law exponents of the low and high frequency flank of the relaxation process, respectively.

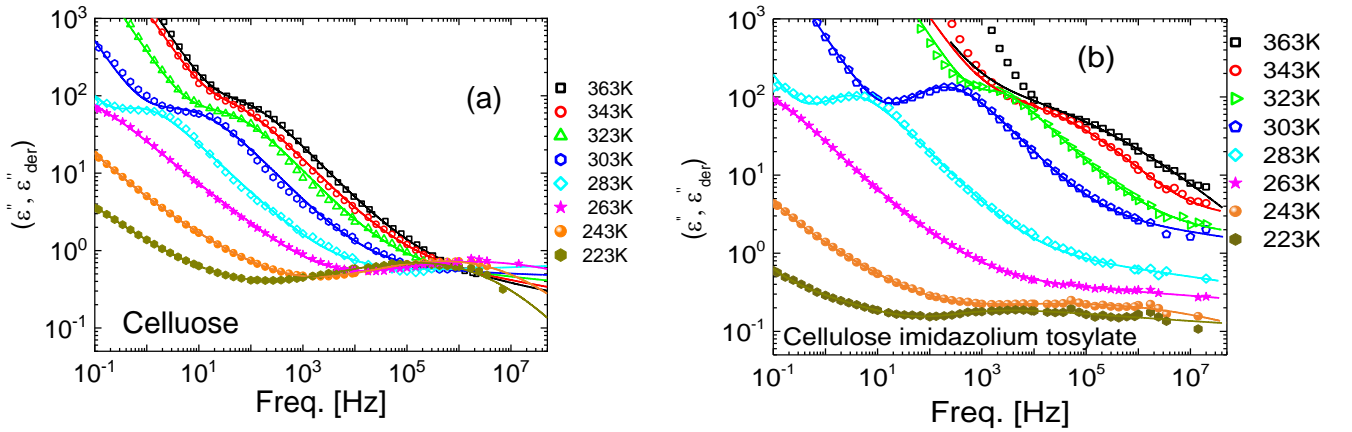


Figure 5: Dielectric imaginary part (loss) obtained from the dielectric real part (open symbols) and as measured (filled symbols) for (a) cellulose and (b) ionocellulose containing imidazolium tosylate at temperatures as indicated. Solid lines are fits along

The γ and β processes are again observed in the modulus spectra in figure 6, which uses $M^*(\nu) = 1/\varepsilon^*(\nu)$. The relaxation times $\tau_\gamma(T)$ and $\tau_\beta(T)$ are obtained using the following equation (Turky, Sangoro, Abdel Rehim, & Kremer, 2010):

$$\tau_{max} = \tau_0 \sin\left(\pi \frac{a}{2+2b}\right)^{-1/a} \sin\left(\pi \frac{ab}{2+2b}\right)^{1/a} \quad (4)$$

The results, $\tau_\gamma(T)$ and $\tau_\beta(T)$ are displayed in figure 8a.

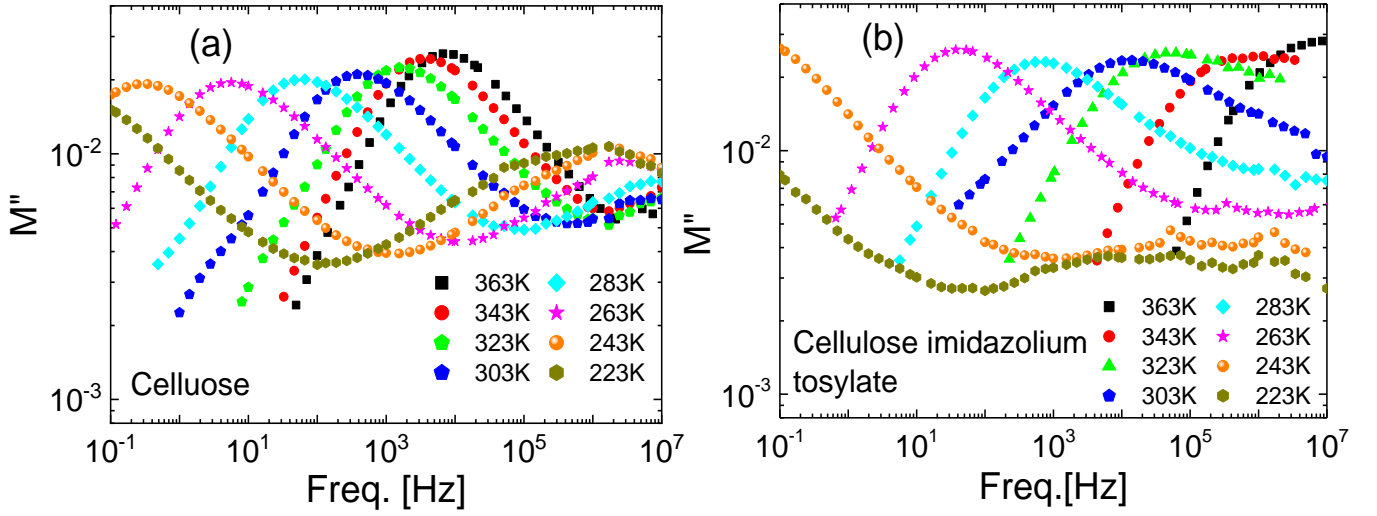


Figure 6: Dielectric modulus imaginary part as a function of frequency of (a) cellulose and (b) ionocellulose containing imidazolium tosylate at temperatures as indicated

The frequency dependence of the real part of the conductivity σ' (ν) for cellulose is displayed in Figure 7a. Three different power-law regimes can be distinguished, similarly to power-law of Jonscher (Jonscher, 1981):

$$\sigma_{ac}(\omega) = \sigma_{dc} + A_1 \omega^{n_1} + A_2 \omega^{n_2} \quad (5)$$

where σ_{dc} defines the *dc* conductivity, A_1 and A_2 are the pre-exponential factor that depend on temperature and material, and n_1 and n_2 are the Jonscher's law exponents. The latter nominates the degree of interaction between mobile ions with the lattices (Gainaru et al., 2016). Regime *I* is almost frequency independent and dominates the measurements at low frequencies. It represents the *dc* conductivity (σ_{dc}) which corresponds to the direct current conductivity. In contrast, the conductivity increases with the frequency in regimes *II* and *III*. Here, the dielectric processes observed in the ϵ'' representation can again be inferred, as shown for other polymeric samples (Hameed, Mohamed, Abdelghany, & Turkey, 2020). Upon cooling, σ_{dc} decreases, and all regimes shift to lower frequency.

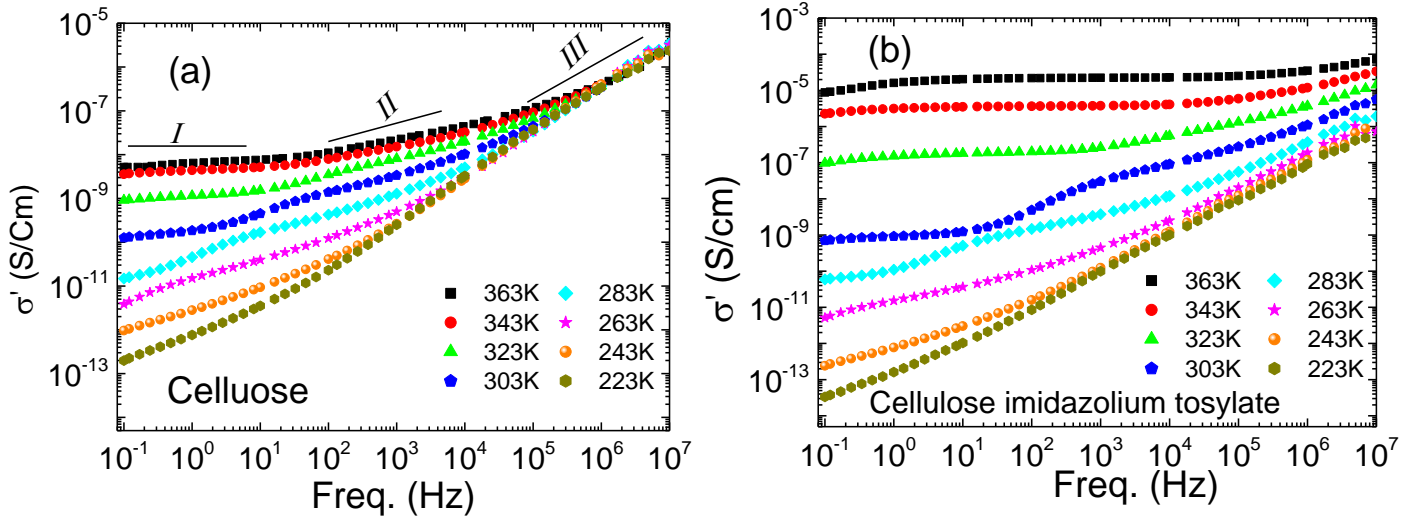


Figure 7: The real part of the conductivity as a function of frequency at temperature as indicated for (a) cellulose and (b) ionocellulose containing imidazolium tosylate. Solid and dashed lines are power-law dependence

For the ionocellulose containing imidazolium tosylate, the $\sigma'(\nu)$ is depicted in figure 7b. The three regimes mentioned before are hardly identified, in particular at high temperatures (*cf.* the data at $T = 363$ K). At high temperature, the measurements are dominated by σ_{dc} (Regime *I*) accompanied by a slight binding at low frequency which is associated with the *EP* effect. Regimes *II* and *III* can again be distinguished at low temperatures. Interestingly, the conductivity is three decades higher than in the case of pure cellulose. The spectral features are similar to those of imidazolium-based ionic liquids (Thomann et al., 2020) or to those of polymer electrolytes in general (Gainaru et al., 2016).

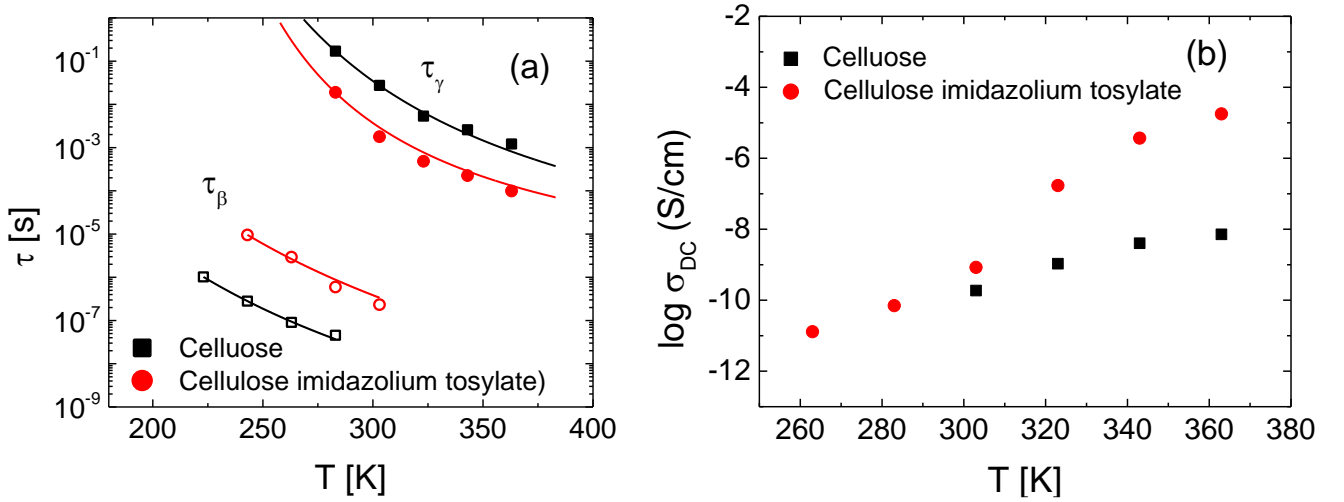


Figure 8: Temperature dependence of (a) the relaxation time (b) the dc conductivity for cellulose and ionocellulose containing imidazolium tosylate.

In figure 8a, the relaxation time $\tau_\gamma(T)$ and $\tau_\beta(T)$ for both neat cellulose and those containing imidazolium tosylate grafts are shown. For both cases, the $\tau_\gamma(T)$ exhibits similar temperature dependence which is well described with Vogel-Fulcher-Tammann (VFT) approach. Yet, the $\tau_\gamma(T)$ are shorter in the case of cellulose containing imidazolium tosylate grafts, which confirms the plasticization effect (Bao et al., 2015; Petridis et al., 2014; Pötzschner et al., 2017). In other words, the attachment of the imidazolium group confers higher flexibility and mobility to the cellulose segments. This may give an indication that the attached imidazolium groups generate a disentanglement effect on cellulose chains on the molecular level. Regarding the relaxation time $\tau_\beta(T)$, an Arrhenius temperature dependence is found for both cases with activation energies of $E_a = 82$ kJ/mol. This is the characteristic behavior of β - processes observed in type B glass formers as well as some polymeric systems (Körber et al., 2017; Mohamed, Hameed, Abdelghany, & Turkey, 2020).

Figure 8b displays the temperature dependence of the dc conductivity $\sigma_{dc}(T)$ for both cases obtained from figure 7. It appears that the dc conductivity at higher temperatures is three orders higher in the case of ionocellulose than in neat cellulose. The ionic conductivity mainly depends on the diffusion of ions and the number of the active ions. Indeed, the electrical conductivity in ionocellulose containing imidazolium tosylate is

related to the anionic tosylate group that is highly mobile at high temperatures. Thus, the significant increase of the conductivity for the ionocellulose containing imidazolium tosylate is possibly correlated to the increase of the number of mobile ionic species within this material.

Finally, the dielectric properties of the ionocellulose mimic those of cellulose nanofibers and cellulose based composite materials (Abdel-karim, Salama, & Hassan, 2018; Tao & Cao, 2020). Thus, the ionocellulose is promising material to replace the traditional dielectric polymer matrices.

4. Conclusion

We report the synthesis of a novel ionocellulose derivative and its characterization using dielectric spectroscopy. Ionic liquids appear as efficient medium for preparing tosylcellulose with high degree of substitution. The obtained tosylcellulose was further reacted with methyl imidazole for producing ionocellulose containing imidazolium tosylate. The imidazolium group is a heterocycle that can be found in numerous biologically relevant compounds such as the essential amino acid histidine, but also in innumerable imidazolium based ionic liquids. The ease of imidazolium derivatization and the huge number of easily accessible imidazolium derivatives pave the way towards a new category of functional ionocellulose materials. The dielectric spectroscopy revealed a presence of two secondary relaxation processes, one is associated to a local motion and the other to localized cooperative molecular mobility in the chain. Introducing the imidazolium tosylate to cellulose enhances the motion which reminds the plasticization effect. Additionally, the conductivity boosted by three order of magnitude. These findings bear great potential for future developments of cellulose in energy storage.

Author statement

Ahmed Salama and Peter Hesemann developed the ionocellulose synthesis and designed the experiments. They shared equally in data curation, funding acquisition, investigation, project administration and writing. Fathia Mohamed measured and discussed all the conductivity measurements. All authors commented on the manuscript and supported data analysis.

Declaration of Competing Interest

The authors declare no competing financial interest.

Acknowledgments

This work was financially supported by the Embassy of France in Egypt – Institut Français d’Egypte (IFE) and Science & Technology Development Fund (STDF) in Egypt.

References

- Abdel-karim, A. M., Salama, A. H., & Hassan, M. L. (2018). Electrical conductivity and dielectric properties of nanofibrillated cellulose thin films from bagasse. *Journal of Physical Organic Chemistry*, 31(9), 1–9. <https://doi.org/10.1002/poc.3851>
- Bao, C. Y., Long, D. R., & Vergelati, C. (2015). Miscibility and dynamical properties of cellulose acetate/plasticizer systems. *Carbohydrate Polymers*, 116, 95–102. <https://doi.org/10.1016/j.carbpol.2014.07.078>
- Bottcher, C. J. F. (1973). *Theory of Electric Polarization*. Elsevier. <https://doi.org/10.1016/C2009-0-15579-4>
- Einfeldt, J., Meißner, D., & Kwasniewski, A. (2001). Polymerdynamics of cellulose and other polysaccharides in solid state-secondary dielectric relaxation processes. *Progress in Polymer Science*, 26(9), 1419–1472. [https://doi.org/10.1016/S0079-6700\(01\)00020-X](https://doi.org/10.1016/S0079-6700(01)00020-X)

- El-Sayed, N. S., El-Sakhawy, M., Hesemann, P., Brun, N., & Kamel, S. (2018). Rational design of novel water-soluble ampholytic cellulose derivatives. *International Journal of Biological Macromolecules*, 114, 363–372. <https://doi.org/10.1016/j.ijbiomac.2018.03.147>
- Elschner, T., & Heinze, T. (2015). Cellulose carbonates: A platform for promising biopolymer derivatives with multifunctional capabilities. *Macromolecular Bioscience*, 15(6), 735–746. <https://doi.org/10.1002/mabi.201400521>
- Gabriel, J., Pabst, F., Helbling, A., Böhmer, T., & Blochowicz, T. (2018). Depolarized Dynamic Light Scattering and Dielectric Spectroscopy: Two Perspectives on Molecular Reorientation in Supercooled Liquids (pp. 203–245). https://doi.org/10.1007/978-3-319-72706-6_7
- Gainaru, C., Stacy, E. W., Bocharova, V., Gobet, M., Holt, A. P., Saito, T., ... Sokolov, A. P. (2016). Mechanism of Conductivity Relaxation in Liquid and Polymeric Electrolytes: Direct Link between Conductivity and Diffusivity. *The Journal of Physical Chemistry B*, 120(42), 11074–11083. <https://doi.org/10.1021/acs.jpcb.6b08567>
- Gericke, M., Schaller, J., Liebert, T., Fardim, P., Meister, F., & Heinze, T. (2012). Studies on the tosylation of cellulose in mixtures of ionic liquids and a co-solvent. *Carbohydrate Polymers*, 89(2), 526–536. <https://doi.org/10.1016/j.carbpol.2012.03.040>
- Hameed, T. A., Mohamed, F., Abdelghany, A. M., & Turkey, G. (2020). Influence of SiO₂ nanoparticles on morphology, optical, and conductivity properties of Poly (ethylene oxide). *Journal of Materials Science: Materials in Electronics*, 31(13), 10422–10436. <https://doi.org/10.1007/s10854-020-03591-5>
- Heinze, T., Talaba, P., & Heinze, U. (2000). Starch derivatives of high degree of functionalization. 1. Effective, homogeneous synthesis of p-toluenesulfonyl (tosyl) starch with a new functionalization pattern. *Carbohydrate Polymers*, 42(4), 411–420. [https://doi.org/10.1016/S0144-8617\(99\)00182-4](https://doi.org/10.1016/S0144-8617(99)00182-4)
- Hofmann, M., Herrmann, A., Abou Elfadl, A., Kruk, D., Wohlfahrt, M., & Rössler, E. A. (2012). Glassy, Rouse, and Entanglement Dynamics As Revealed by Field Cycling 1 H NMR Relaxometry. *Macromolecules*, 45(5), 2390–2401.

<https://doi.org/10.1021/ma202371p>

- Jafarpour, G., Dantras, E., Boudet, A., & Lacabanne, C. (2007). Study of dielectric relaxations in cellulose by combined DDS and TSC. *Journal of Non-Crystalline Solids*, 353(44–46), 4108–4115. <https://doi.org/10.1016/j.jnoncrysol.2007.06.026>
- Jafarpour, G., Dantras, E., Boudet, A., & Lacabanne, C. (2008). Molecular mobility of poplar cell wall polymers studied by dielectric techniques. *Journal of Non-Crystalline Solids*, 354(27), 3207–3214. <https://doi.org/10.1016/j.jnoncrysol.2008.01.008>
- Jonscher, A. K. (1981). A new understanding of the dielectric relaxation of solids. *Journal of Materials Science*, 16(8), 2037–2060. <https://doi.org/10.1007/BF00542364>
- Kadokawa, J., Murakami, M., & Kaneko, Y. (2008). A facile preparation of gel materials from a solution of cellulose in ionic liquid. *Carbohydrate Research*, 343(4), 769–772. <https://doi.org/10.1016/j.carres.2008.01.017>
- Kaminski, K., Kaminska, E., Hensel-Bielowka, S., Chelmecka, E., Paluch, M., Ziolo, J., ... Ngai, K. L. (2008). Identification of the Molecular Motions Responsible for the Slower Secondary (β) Relaxation in Sucrose. *The Journal of Physical Chemistry B*, 112(25), 7662–7668. <https://doi.org/10.1021/jp711502a>
- Kaminski, K., Kaminska, E., Ngai, K. L., Paluch, M., Włodarczyk, P., Kasprzycka, A., & Szeja, W. (2009). Identifying the Origins of Two Secondary Relaxations in Polysaccharides. *The Journal of Physical Chemistry B*, 113(30), 10088–10096. <https://doi.org/10.1021/jp809760t>
- Körber, T., Mohamed, F., Hofmann, M., Lichtinger, A., Willner, L., & Rössler, E. A. (2017). The Nature of Secondary Relaxations: The Case of Poly(ethylene- alt -propylene) Studied by Dielectric and Deuteron NMR Spectroscopy. *Macromolecules*, 50(4), 1554–1568. <https://doi.org/10.1021/acs.macromol.6b02536>
- Koschella, A., Hartlieb, M., & Heinze, T. (2011). A “click-chemistry” approach to cellulose-based hydrogels. *Carbohydrate Polymers*, 86(1), 154–161. <https://doi.org/10.1016/j.carbpol.2011.04.031>

- Lai, W.-F., & Lin, M. C.-M. (2009). Nucleic acid delivery with chitosan and its derivatives. *Journal of Controlled Release*, 134(3), 158–168.
<https://doi.org/10.1016/j.jconrel.2008.11.021>
- Liu, C., & Baumann, H. (2005). New 6-butylamino-6-deoxycellulose and 6-deoxy-6-pyridiniumcellulose derivatives with highest regioselectivity and completeness of reaction, 340, 2229–2235. <https://doi.org/10.1016/j.carres.2005.07.018>
- Liu, S., Liu, J., Esker, A. R., & Edgar, K. J. (2016). An Efficient, Regioselective Pathway to Cationic and Zwitterionic N-Heterocyclic Cellulose Ionomers. *Biomacromolecules*, 17(2), 503–513.
<https://doi.org/10.1021/acs.biomac.5b01416>
- Minnick, D. L., Flores, R. A., & Scurto, A. M. (2017). Viscosity and Rheology of Ionic Liquid Mixtures Containing Cellulose and Cosolvents for Advanced Processing (pp. 189–208). <https://doi.org/10.1021/bk-2017-1250.ch008>
- Mohamed, F., Flämig, M., Hofmann, M., Heymann, L., Willner, L., Fatkullin, N., ... Rössler, E. A. (2018). Scaling analysis of the viscoelastic response of linear polymers. *The Journal of Chemical Physics*, 149(4), 044902.
<https://doi.org/10.1063/1.5038643>
- Mohamed, F., Hameed, T. A., Abdelghany, A. M., & Turkey, G. (2020). Structure–dynamic properties relationships in poly(ethylene oxide)/silicon dioxide nanocomposites: dielectric relaxation study. *Polymer Bulletin*.
<https://doi.org/10.1007/s00289-020-03368-0>
- Nusser, K., Schneider, G. J., & Richter, D. (2011). Microscopic origin of the terminal relaxation time in polymer nanocomposites: an experimental precedent. *Soft Matter*, 7(18), 7988. <https://doi.org/10.1039/c1sm05555k>
- Petridis, L., O'Neill, H. M., Johnsen, M., Fan, B., Schulz, R., Mamontov, E., ... Smith, J. C. (2014). Hydration Control of the Mechanical and Dynamical Properties of Cellulose. *Biomacromolecules*, 15(11), 4152–4159.
<https://doi.org/10.1021/bm5011849>
- Pötzschner, B., Mohamed, F., Bächer, C., Wagner, E., Lichtinger, A., Minikejew, R., ... Rössler, E. A. (2017). Non-polymeric asymmetric binary glass-formers. I.

- Main relaxations studied by dielectric, ²H NMR, and ³¹P NMR spectroscopy. *The Journal of Chemical Physics*, 146(16), 164504.
<https://doi.org/10.1063/1.4980084>
- Rahn, K., Diamantoglou, M., Klemm, D., Berghmans, H., & Heinze, T. (1996). Homogeneous synthesis of cellulose p-toluenesulfonates in N,N-dimethylacetamide/LiCl solvent system. *Die Angewandte Makromolekulare Chemie*, 238, 143–163. <https://doi.org/10.1002/apmc.1996.052380113>
- Rong, L., Zeng, M., Liu, H., Wang, B., Mao, Z., & Xu, H. (2019). Biginelli reaction on cellulose acetoacetate : a new approach for versatile cellulose derivatives. *Carbohydrate Polymers*, 209(2999), 223–229.
<https://doi.org/10.1016/j.carbpol.2019.01.036>
- Salama, A. (2019). Cellulose/calcium phosphate hybrids: New materials for biomedical and environmental applications. *International Journal of Biological Macromolecules*, 127, 606–617. <https://doi.org/10.1016/j.ijbiomac.2019.01.130>
- Salama, A., Abou-Zeid, R. E., Cruz-Maya, I., & Guarino, V. (2020). Soy protein hydrolysate grafted cellulose nanofibrils with bioactive signals for bone repair and regeneration. *Carbohydrate Polymers*, 229(August 2019), 115472.
<https://doi.org/10.1016/j.carbpol.2019.115472>
- Salama, A., & El-Sakhawy, M. (2016). Regenerated cellulose/wool blend enhanced biomimetic hydroxyapatite mineralization. *International Journal of Biological Macromolecules*, 92, 920–925. <https://doi.org/10.1016/j.ijbiomac.2016.07.077>
- Salama, A., Hasanin, M., & Hesemann, P. (2020). Synthesis and antimicrobial properties of new chitosan derivatives containing guanidinium groups. *Carbohydrate Polymers*, 241, 116363.
<https://doi.org/10.1016/j.carbpol.2020.116363>
- Salama, A., & Hesemann, P. (2018a). New N-guanidinium chitosan/silica ionic microhybrids as efficient adsorbent for dye removal from waste water. *International Journal of Biological Macromolecules*, 111, 762–768.
<https://doi.org/10.1016/j.ijbiomac.2018.01.049>
- Salama, A., & Hesemann, P. (2018b). Synthesis of N-Guanidinium-chitosan/silica

- hybrid composites: Efficient adsorbents for anionic pollutants. *Journal of Polymers and the Environment*, 26(5), 1986–1997.
<https://doi.org/10.1007/s10924-017-1093-3>
- Salama, A., & Hesemann, P. (2020a). Recent Trends in Elaboration, Processing, and Derivatization of Cellulosic Materials Using Ionic Liquids. *ACS Sustainable Chemistry & Engineering*, 8, 17893–17907.
<https://doi.org/10.1021/acssuschemeng.0c06913>
- Salama, A., & Hesemann, P. (2020b). Synthesis and characterization of N - guanidinium chitosan / silica ionic hybrids as templates for calcium phosphate mineralization. *International Journal of Biological Macromolecules*, 147, 276–283. <https://doi.org/10.1016/j.ijbiomac.2020.01.046>
- Salama, A., Neumann, M., Günter, C., & Taubert, A. (2014). Ionic liquid-assisted formation of cellulose/calcium phosphate hybrid materials. *Beilstein Journal of Nanotechnology*, 5, 1553–1568. <https://doi.org/10.3762/bjnano.5.167>
- Sawada, A. (2007). Theory of space-charge polarization for determining ionic constants of electrolytic solutions. *The Journal of Chemical Physics*, 126(22), 224515. <https://doi.org/10.1063/1.2741254>
- Schmidt, S., Liebert, T., & Heinze, T. (2014). Synthesis of soluble cellulose tosylates in an eco-friendly medium. *Green Chem.*, 16, 1941–1946.
<https://doi.org/10.1039/c3gc41994k>
- Tao, J., & Cao, S. (2020). Flexible high dielectric thin films based on cellulose nanofibrils and acid oxidized multi-walled carbon nanotubes. *RSC Advances*, 10(18), 10799–10805. <https://doi.org/10.1039/C9RA10915C>
- Thanou, M., Verhoef, J. ., & Junginger, H. . (2001). Chitosan and its derivatives as intestinal absorption enhancers. *Advanced Drug Delivery Reviews*, 50, S91–S101. [https://doi.org/10.1016/S0169-409X\(01\)00180-6](https://doi.org/10.1016/S0169-409X(01)00180-6)
- Thomann, C. A., Münzner, P., Moch, K., Jacquemin, J., Goodrich, P., Sokolov, A. P., ... Gainaru, C. (2020). Tuning the dynamics of imidazolium-based ionic liquids via hydrogen bonding. I. The viscous regime. *The Journal of Chemical Physics*, 153(19), 194501. <https://doi.org/10.1063/5.0026144>

- Turky, G., Sangoro, J. R., Abdel Rehim, M., & Kremer, F. (2010). Secondary relaxations and electrical conductivity in hyperbranched polyester amides. *Journal of Polymer Science Part B: Polymer Physics*, 48(14), 1651–1657. <https://doi.org/10.1002/polb.21966>
- Wang, H., Gurau, G., & Rogers, R. D. (2012). Ionic liquid processing of cellulose. *Chemical Society Reviews*, 41(4), 1519–1537. <https://doi.org/10.1039/c2cs15311d>
- Wieland, F., Bocharova, V., Münzner, P., Hiller, W., Sakrowski, R., Sternemann, C., ... Gainaru, C. (2019). Structure and dynamics of short-chain polymerized ionic liquids. *The Journal of Chemical Physics*, 151(3), 034903. <https://doi.org/10.1063/1.5109228>
- Wu, J., Zhang, J., Zhang, H., He, J., Ren, Q., & Guo, M. (2004). Homogeneous acetylation of cellulose in a new ionic liquid. *Biomacromolecules*, 5(2), 266–268. <https://doi.org/10.1021/bm034398d>
- Wübbenhorst, M., & van Turnhout, J. (2002). Analysis of complex dielectric spectra. I. One-dimensional derivative techniques and three-dimensional modelling. *Journal of Non-Crystalline Solids*, 305(1–3), 40–49. [https://doi.org/10.1016/S0022-3093\(02\)01086-4](https://doi.org/10.1016/S0022-3093(02)01086-4)